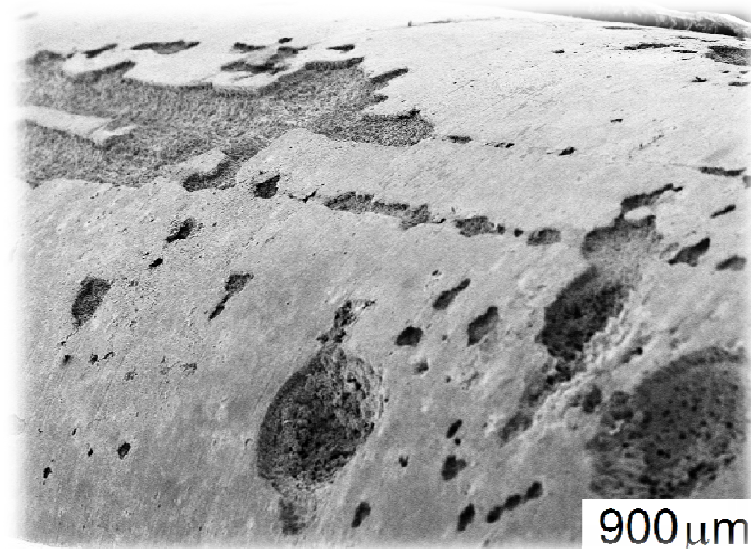


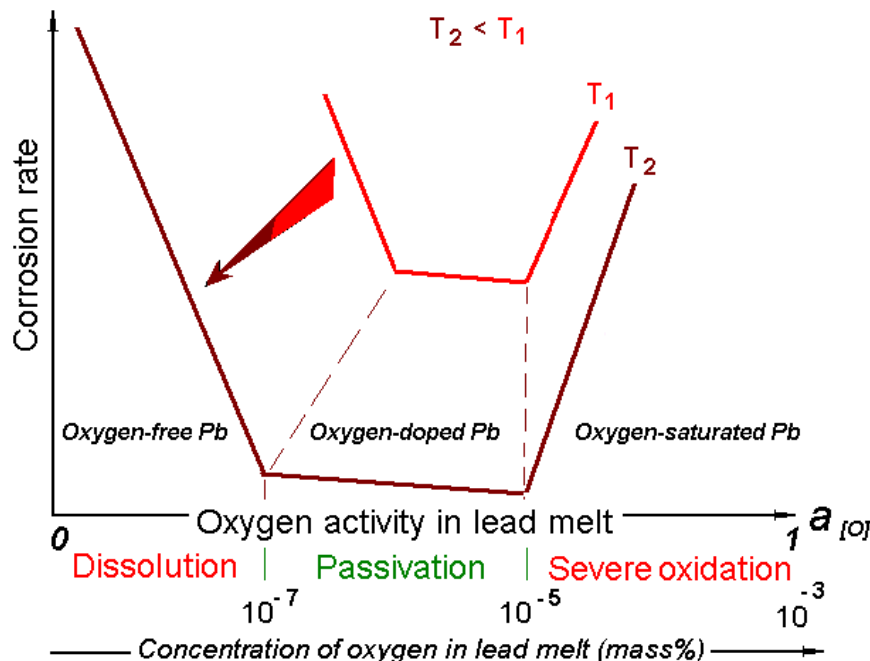
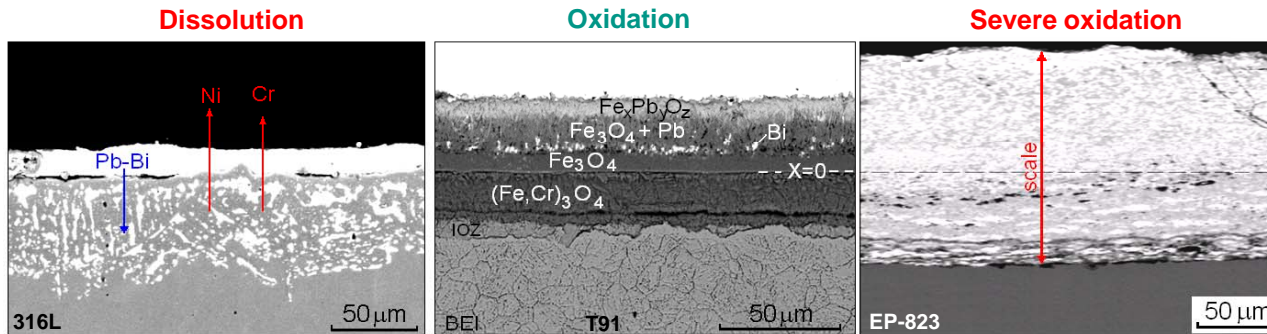
Corrosion behavior of austenitic steels 1.4970, 316L and 1.4571 in flowing LBE at 450 and 550°C with 10^{-7} mass % dissolved oxygen

Valentyn Tsisar, Carsten Schroer, Olaf Wedemeyer, Aleksandr Skrypnik, Jürgen Konys

INSTITUTE FOR APPLIED MATERIALS – MATERIAL PROCESS TECHNOLOGY (IAM-WPT)



In-situ technology of Pb and Pb-Bi melt doping with oxygen in order to form the protective oxide layer on the surface of steel



Schematic representation of corrosion rate and interaction modes of steels in Pb/Pb-Bi melts depending on the oxygen concentration in the liquid metal and temperature.

BASIS of Pb-Bi technology

- ❑ Pb / Pb-Bi dissolves and transports the oxygen;
- ❑ Components of steels (Si, Cr, Fe...) have high affinity to oxygen than Pb or Bi.

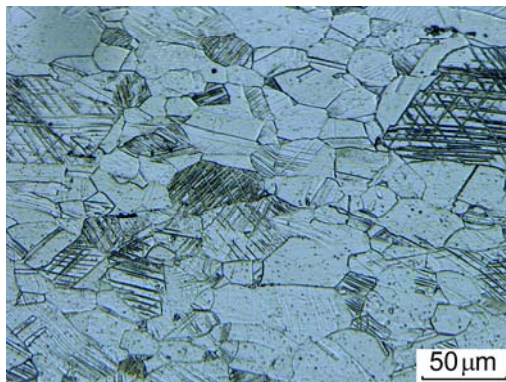
1.1 Materials



(Fe – Bal.)

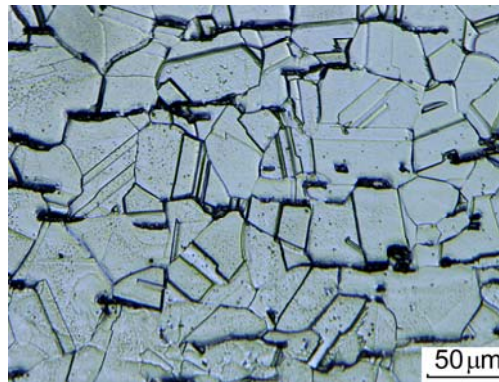
Austenitic steels	Cr	Ni	Mo	Mn	Si	Cu	V	W	Al	Ti	C	N	P	S	B
316L	16.73	9.97	2.05	1.81	0.67	0.23	0.07	0.02	0.018	-	0.019	0.029	0.032	0.0035	-
1.4970	15.95	15.4	1.2	1.49	0.52	0.026	0.036	< 0.005	0.023	0.44	0.1	0.009	< 0.01	0.0036	< 0.01
1.4571	17.50	12	2.0	2.0	1.0	-	-	-	-	0.70	0.08	-	0.045	0.015	-

1.4970 (15-15Ti)



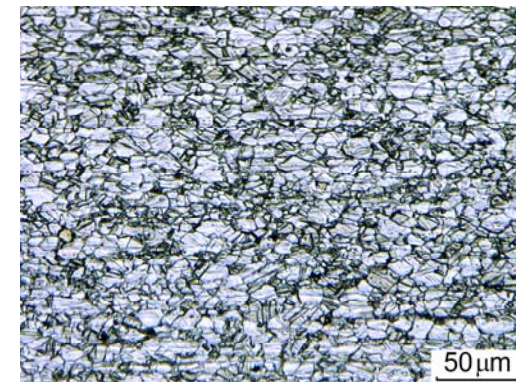
- HV₃₀ = 253;
- Grain size ranged from 20 to 65 μm;
- Intersecting deformation twins.

316L



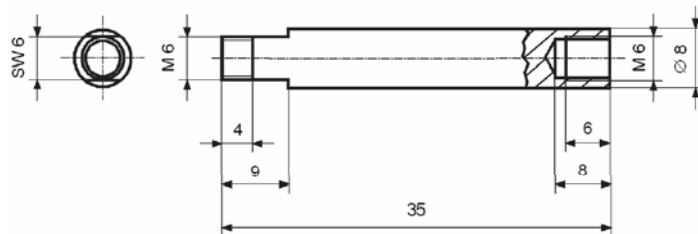
- HV₃₀ = 132;
- Grain size averaged 50 μm (G 5.5);
- Annealing twins.

1.4571

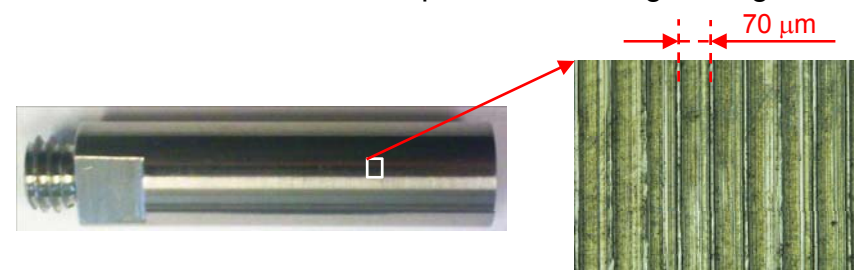


- HV₃₀ = 245;
- Grain size averaged 50 μm (G 9.5).

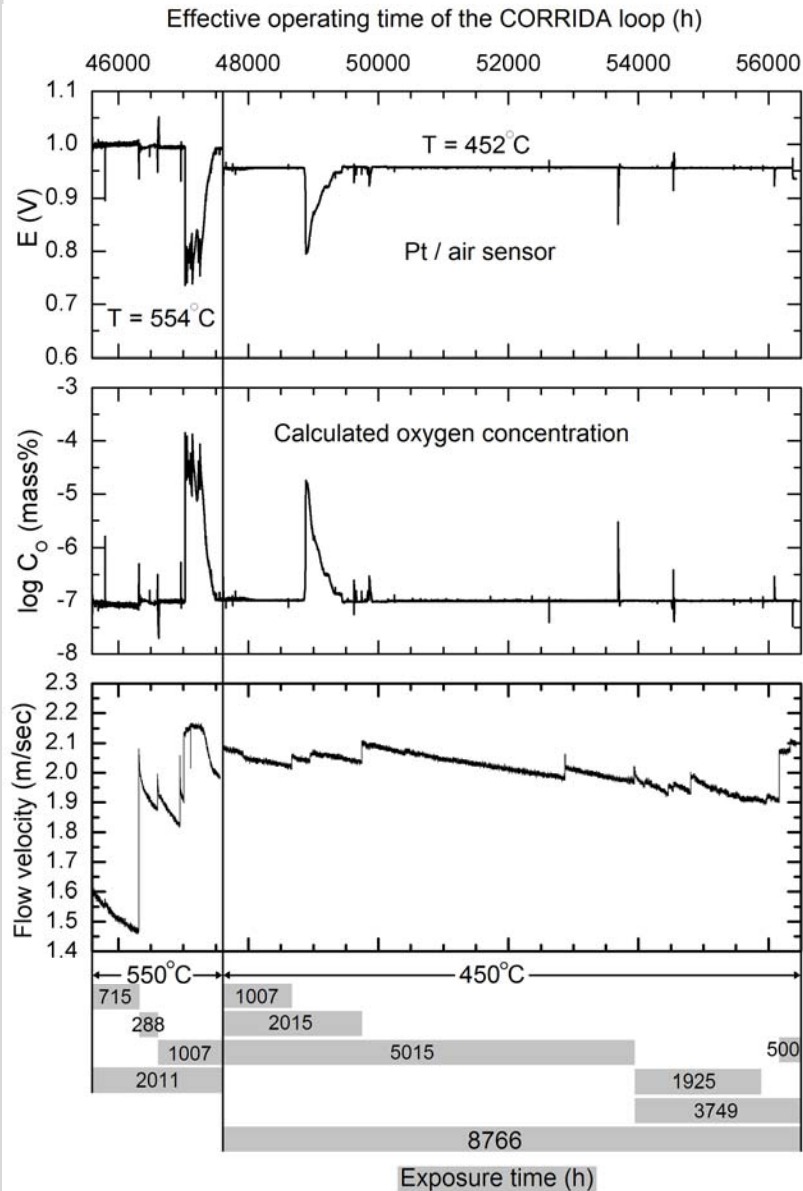
Shape and dimensions of sample for corrosion tests



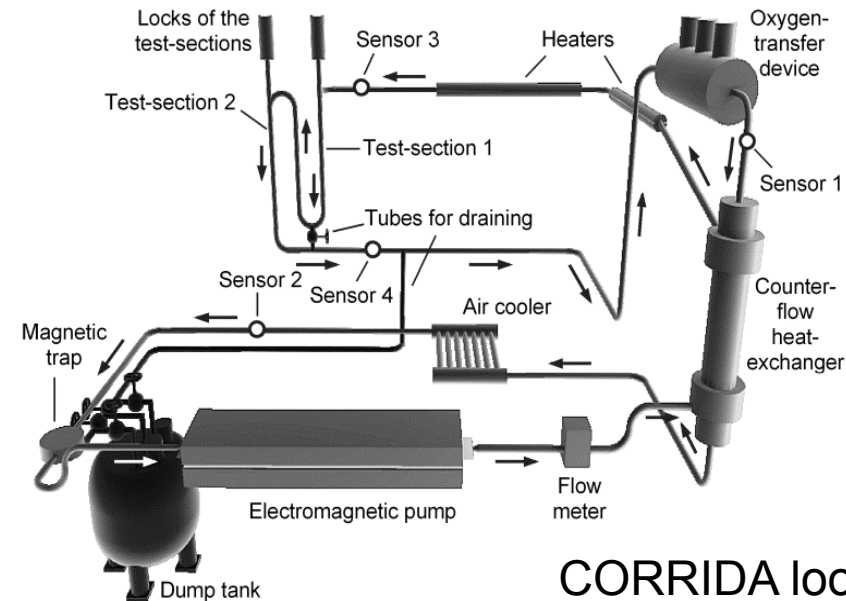
General view of initial sample after finishing turning



Test parameters



- **T = 550(+5)°C**
 $T_{\min} \approx 385^{\circ}\text{C}$
 $C_{\text{O}} = 10^{-7}$ mass%, excursion to 10^{-4} – 10^{-5} mass%O
 $v = 2(+/-0.2)$ m/s, initially 1.5–1.6 m/s
 $t = 288; 715; 1007; 2011$ h
- **T = 450(+5)°C**
 $T_{\min} \approx 350^{\circ}\text{C}$
 $C_{\text{O}} = 10^{-7}$ mass%, excursion to 10^{-5} mass% O
 $v = 2(+/-0.2)$ m/s
 $t = 500; 1007; 1925; 2015; 3749; 5015; 8766$ h



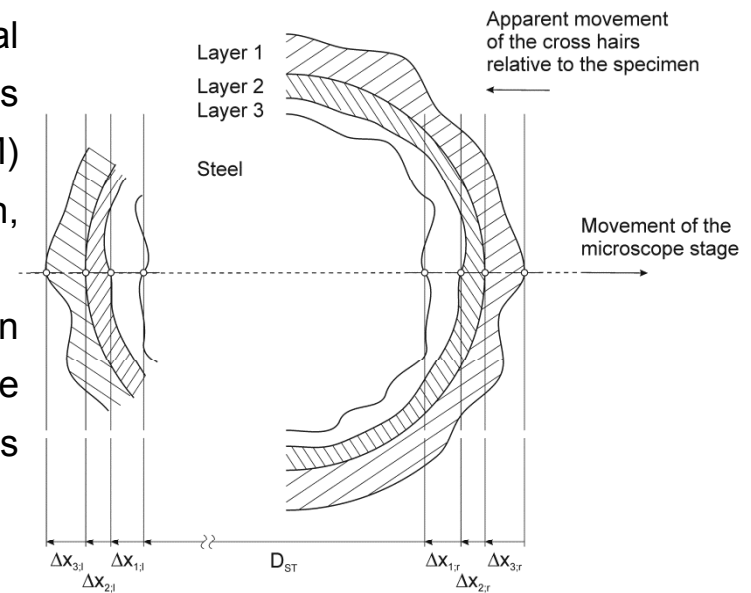
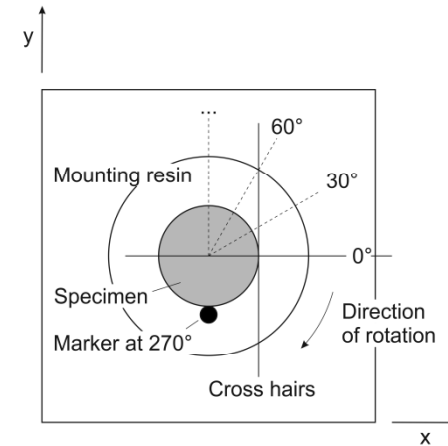
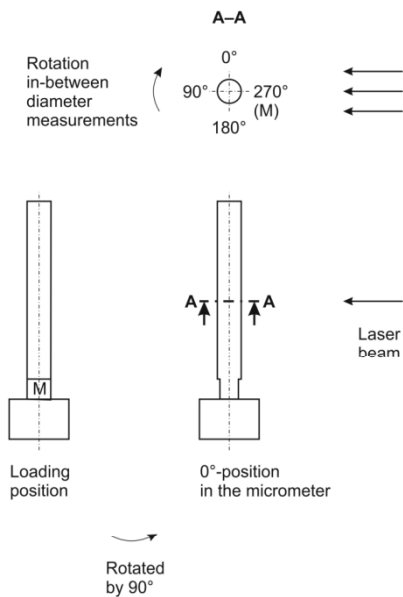
Quantification of corrosion

Goal of quantification

- Material loss, average of general corrosion and maximum of local corrosion
- Thickness of adherent (oxide) scale
- Overall change in dimensions, including the scale
- Amount of metals transferred to the liquid metal

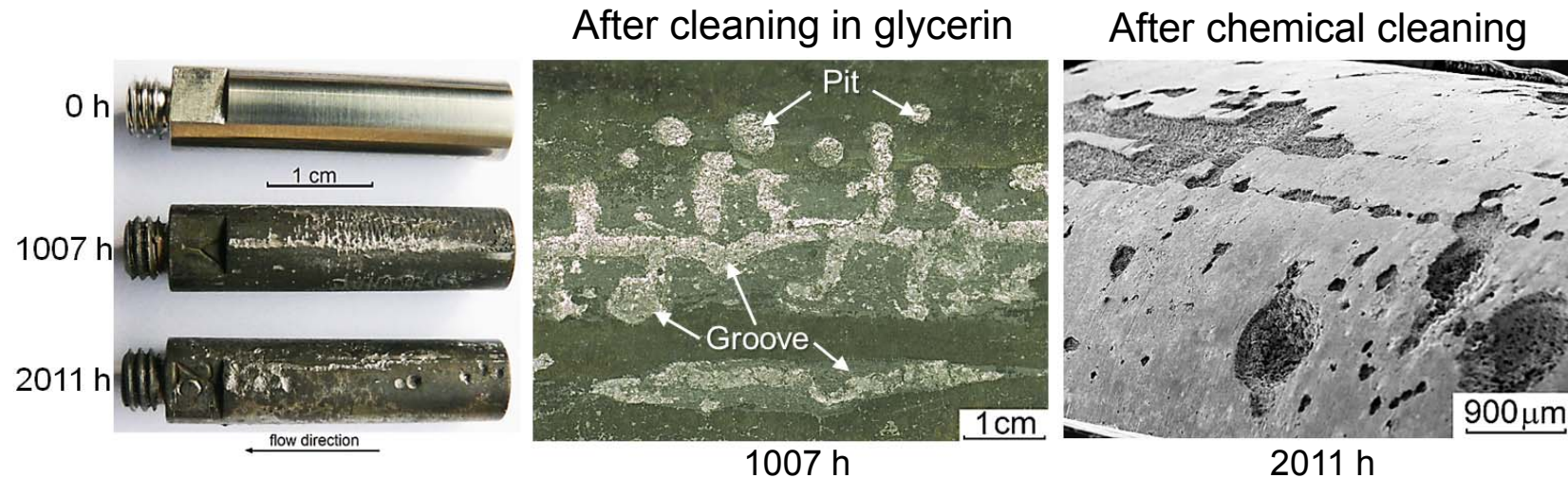
Metallographic method (cylindrical specimens)

- Measurement of initial diameter in a laser micrometer with 0.1 μm resolution
- Diameter of unaffected material and thickness of corrosion scales determined in a microscope (LOM) at minimum $\times 500$ magnification, with 1 μm resolution
- Occurrence of different corrosion modes on opposing sides of the re-measured diameter is considered in the evaluation



Quantification of corrosion modes on surface of austenitic steels after exposure to flowing LBE at 450/550°C, 2 m/s with 10⁻⁷ mass% O

General surface topography of austenitic steels (1.4970) after test at 550°C



Surface appearance:

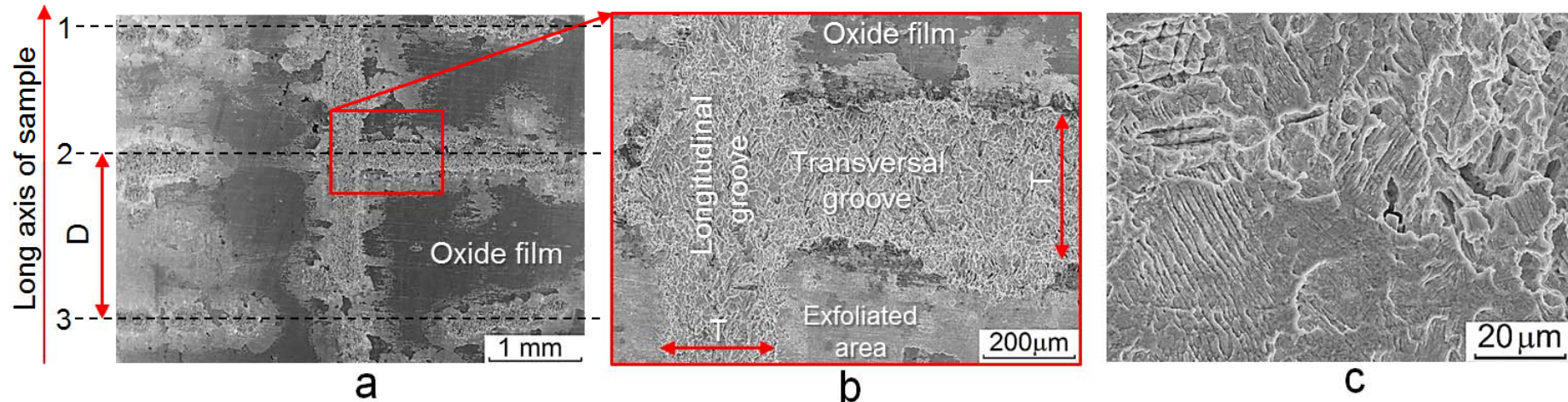
- Green-colored oxide film;
- Light areas with exfoliated oxide film;
- Zones of severe local corrosion attack:
 - hemispherical pits;
 - longitudinal and transversal grooves;
- The percentage of surface covered by the oxide film decreases with exposure time in LBE, while the number of sites affected by local corrosion attack respectively increases.

General surface topography of austenitic steels (1.4970) after test at 450°C for 5015 h

Segment of sample is chemically cleaned

Macro-defects

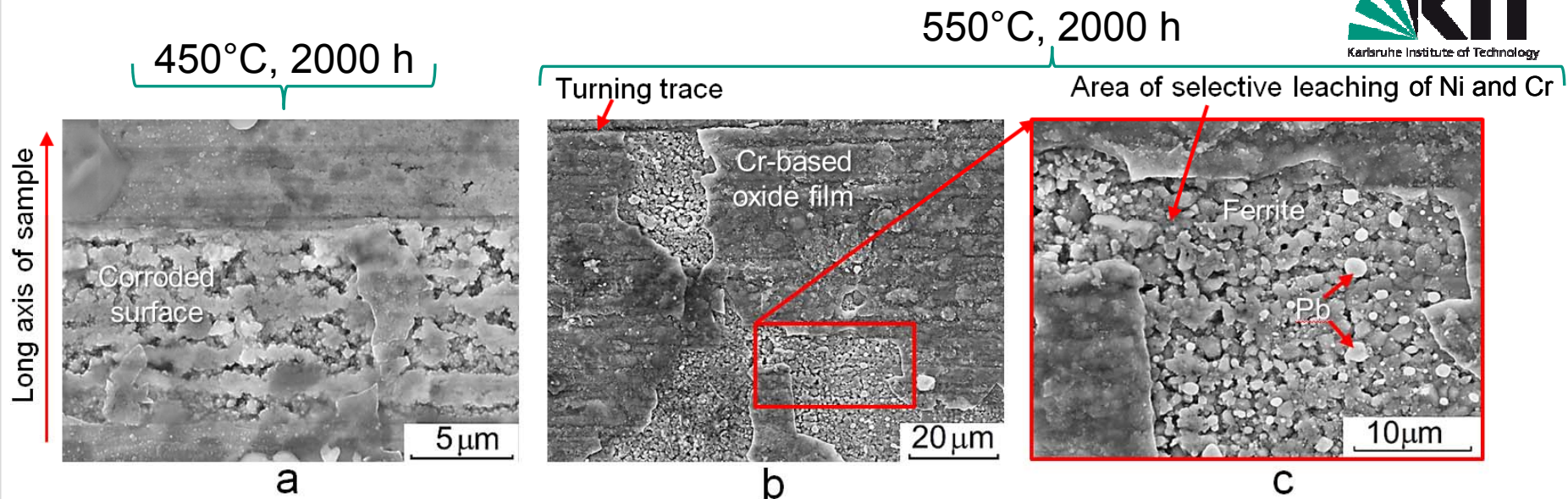
Micro-defects



Macro-defects:

- ❑ Intersecting corrosion grooves;
- ❑ Grooves form regular network-like structure characterized by similar and repetitive dimensional parameters which could be associated with final finishing turning (a, b);
- ❑ Pre-existing active paths, i.e. grains and/or sub-grain boundaries and twins are the main paths for selective leaching of Ni and Cr and subsequent penetration of Pb and Bi into steel matrix.

Surface examination of tested steels (1.4970)

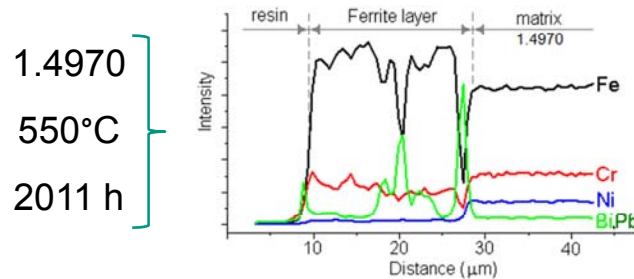
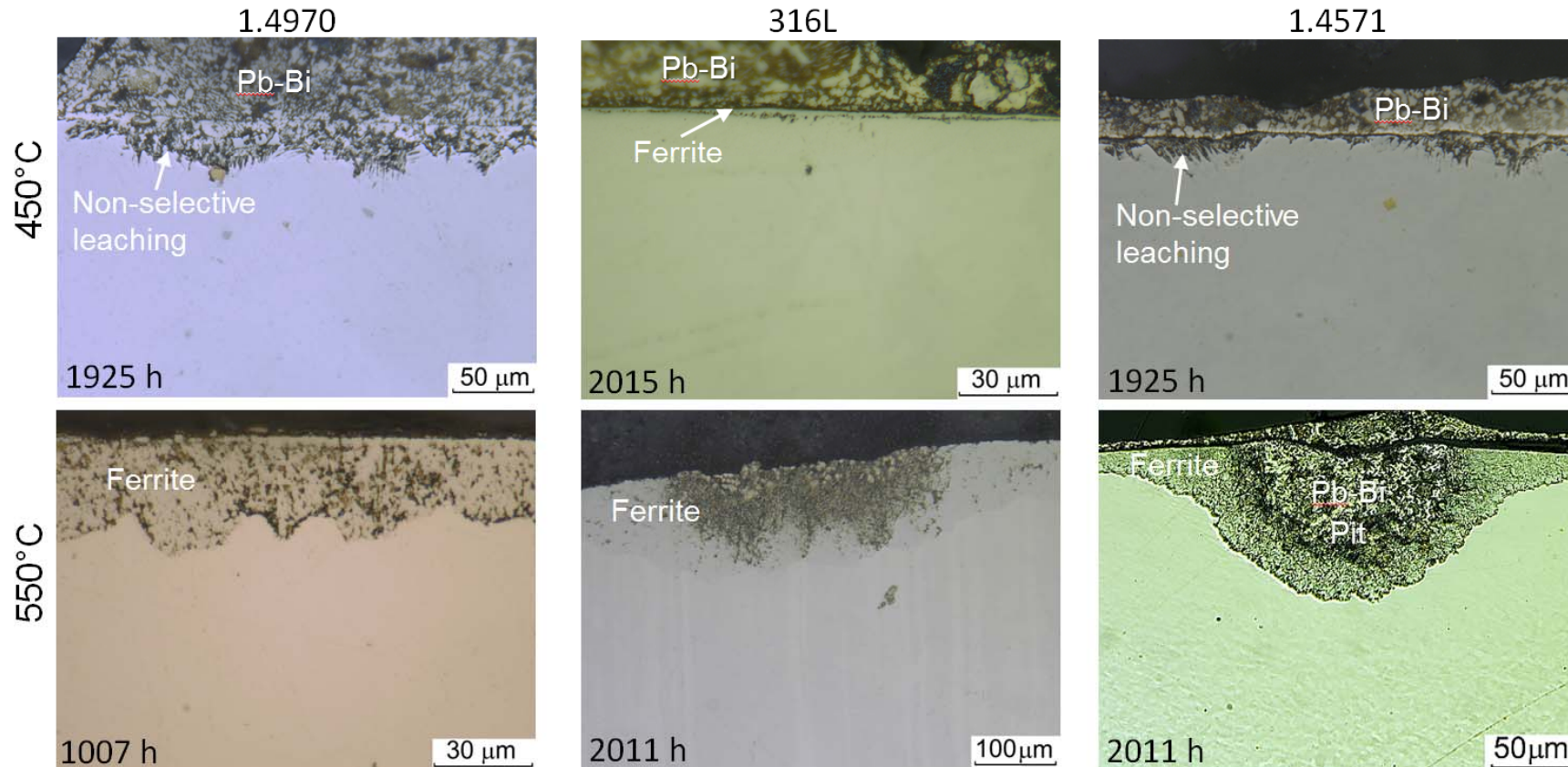


T (°C)	mass %	O	Si	Ti	Cr	Fe	Ni	Pb	Bi
450	Surface area scan (a)	15.89	0.84	0.58	19.84	48.91	10.39	2.38	1.17
	Corroded surface (a)	-	0.61	0.07	6.58	42.25	4.00	22.70	23.79
550	Cr-based oxide film (b)	31.89	0.63	0.55	39.05	19.39	0.22	3.50	4.78
	Ferrite (c)	-	0.77	0.28	12.92	78.21	0.84	1.73	3.42

- ❑ Surface of austenitic steels are covered by thin ($\leq 0.5 \mu\text{m}$) Cr-based oxide film;
- ❑ Porous corroded surface markedly depleted in Cr and Ni and penetrated with Pb and Bi is also observed.

Cross-section examination of tested steels

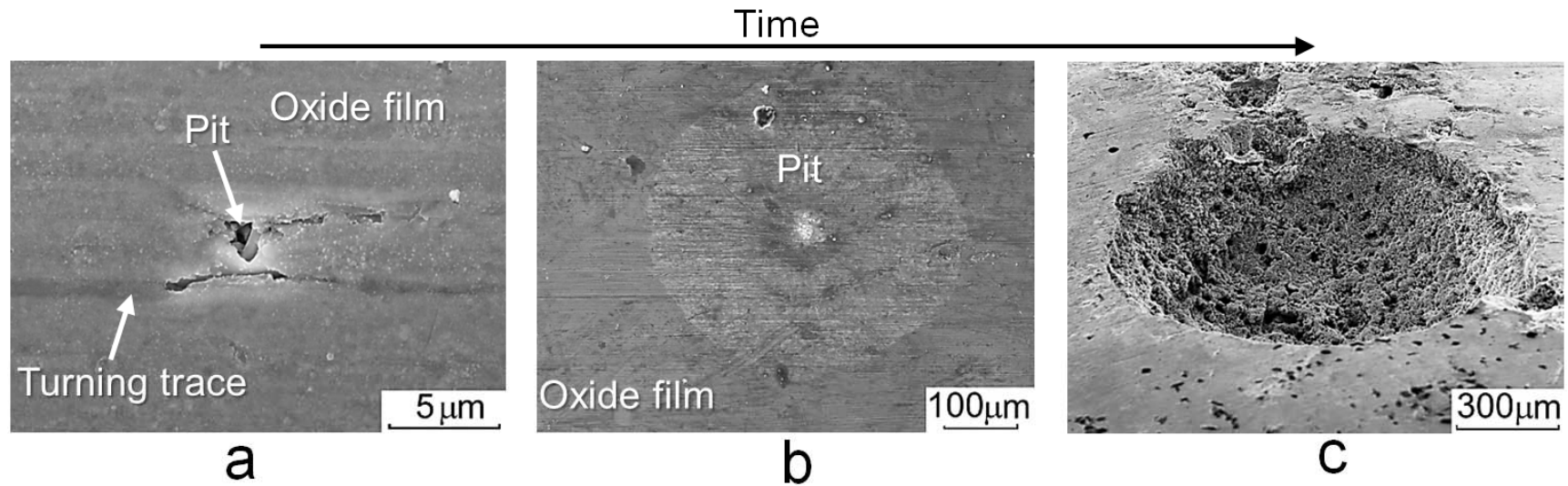
Layer-type attack - formation of ferrite layer depleted in Ni and Cr and penetrated by Pb and Bi



Steel	Ferrite layer composition (mass %)				
	Ni	Cr	Fe	Pb	Bi
1.4970	1.85	6.76	84.47	-	3.12
316L	1.10	8.13	86.48	-	1.95
1.4571	1.61	6.15	69.15	6.45	13.75

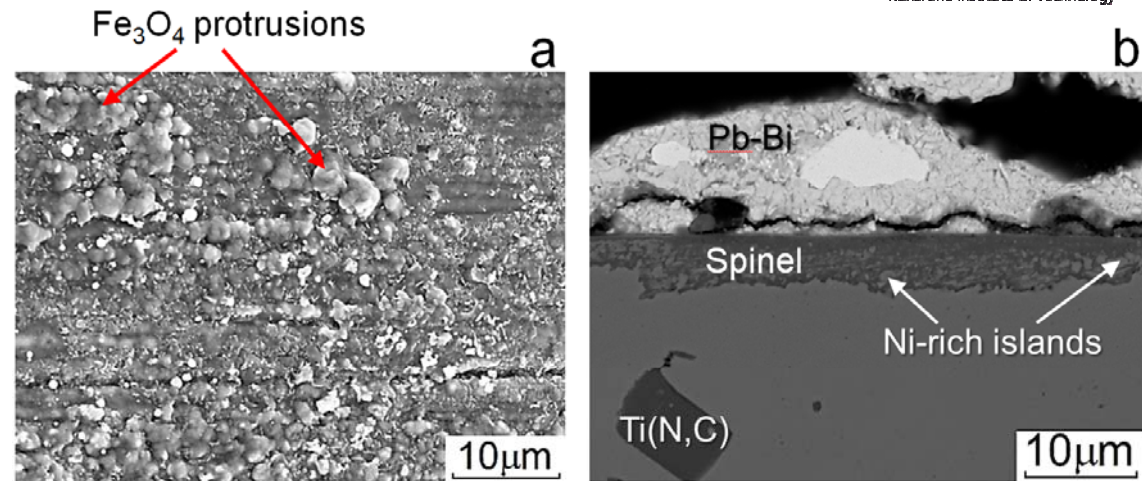
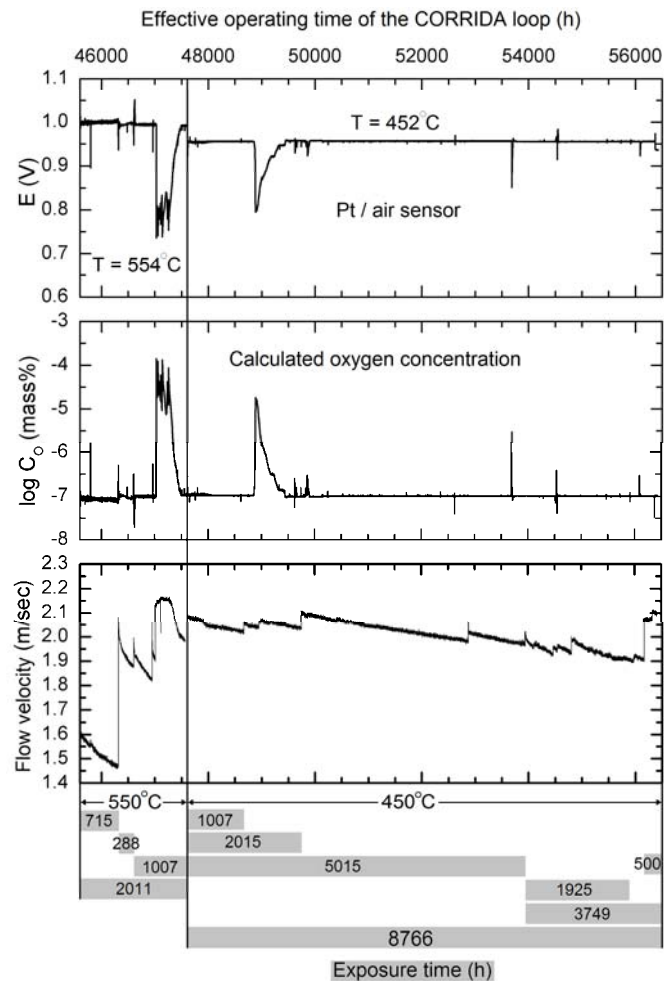
Local pit-type corrosion attack

Expected sequence of evolution of corrosion pits with time



Object analyzed	mass %					
	O	Cr	Fe	Ni	Pb	Bi
Oxide film (a)	10.68	16.36	54.06	14.57	1.86	1.30
Oxide film (b)	7.21	16.08	63.17	10.23	2.21	-
Pit (b)	13.95	8.90	29.62	0.97	5.87	40.49

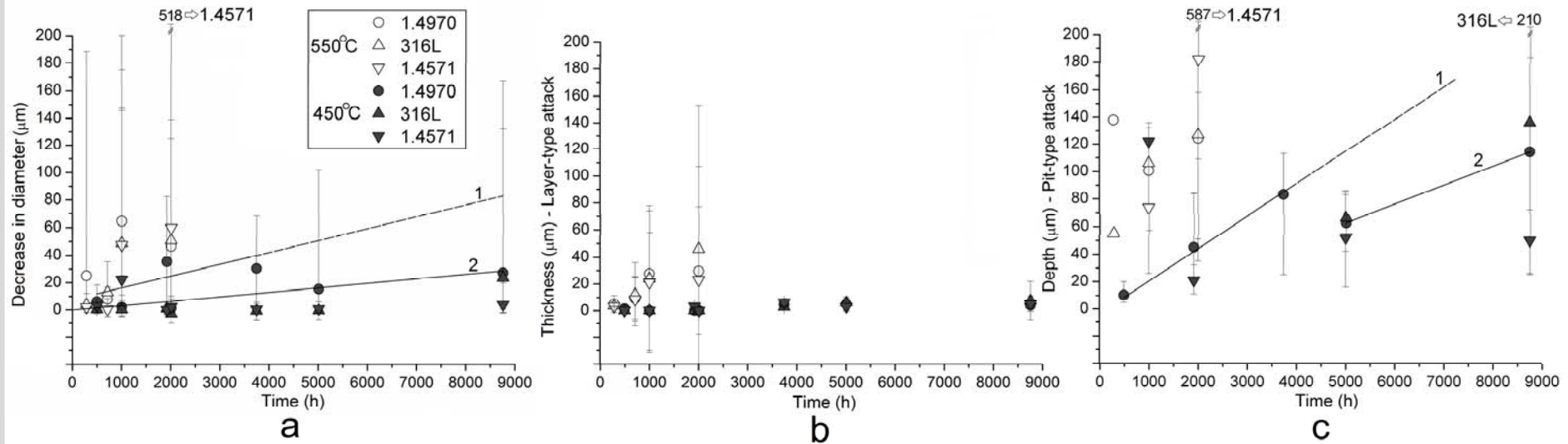
Effect of temporal increase in oxygen concentration



Object analyzed	mass %			
	O	Cr	Fe	Ni
Protrusions	27.63	2.46	69.43	-
Spinel	21.16	25.21	38.70	2.89
Ni-rich islands	2.85	8.96	59.73	20.05

- ❑ Growth of rare magnetite protrusions on the surface of 316L steel (550°C, 1007 h) (Fig. a);
- ❑ Formation of islands of Fe-Cr spinel (1.4970 exposed at 550°C (Fig. b).

Quantification of corrosion loss of austenitic steels after exposure to flowing LBE at 450/550°C, 2 m/s with 10^{-7} mass% O



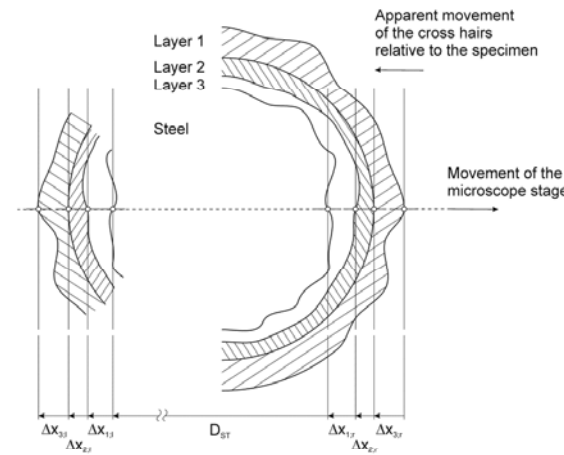
450°C:

- ❑ Corrosion loss measured as decrease in diameter does not exceed 4, 27, and 26 μm after 8766 h for 1.4571, 1.4970 and 316L steels, respectively;
- ❑ Thickness of layer-type attack (ferrite) averaged 5, 7 and 4 μm after 8766 h for 1.4571, 1.4970 and 316L steels, respectively;
- ❑ Depth of pit-type attack average 50, 114 and 136 μm correspondingly. The percentage of circumference affected by selective leaching increases with time and after 8766 h reached 100 %.

550°C:

- ❑ Decrease in diameter averaged ~ 60 , 46 and 51 μm after 2011 h for 1.4571, 1.4970 and 316L steels, respectively;
- ❑ Layer-type attack averaged 23, 30 and 46 μm ;
- ❑ Depth of pit-type attack averaged 182, 124 and 127 μm .

Percentage of circumference affected by selective leaching attack that resulted in either formation of layer-type (L) or pit-type (P) damage



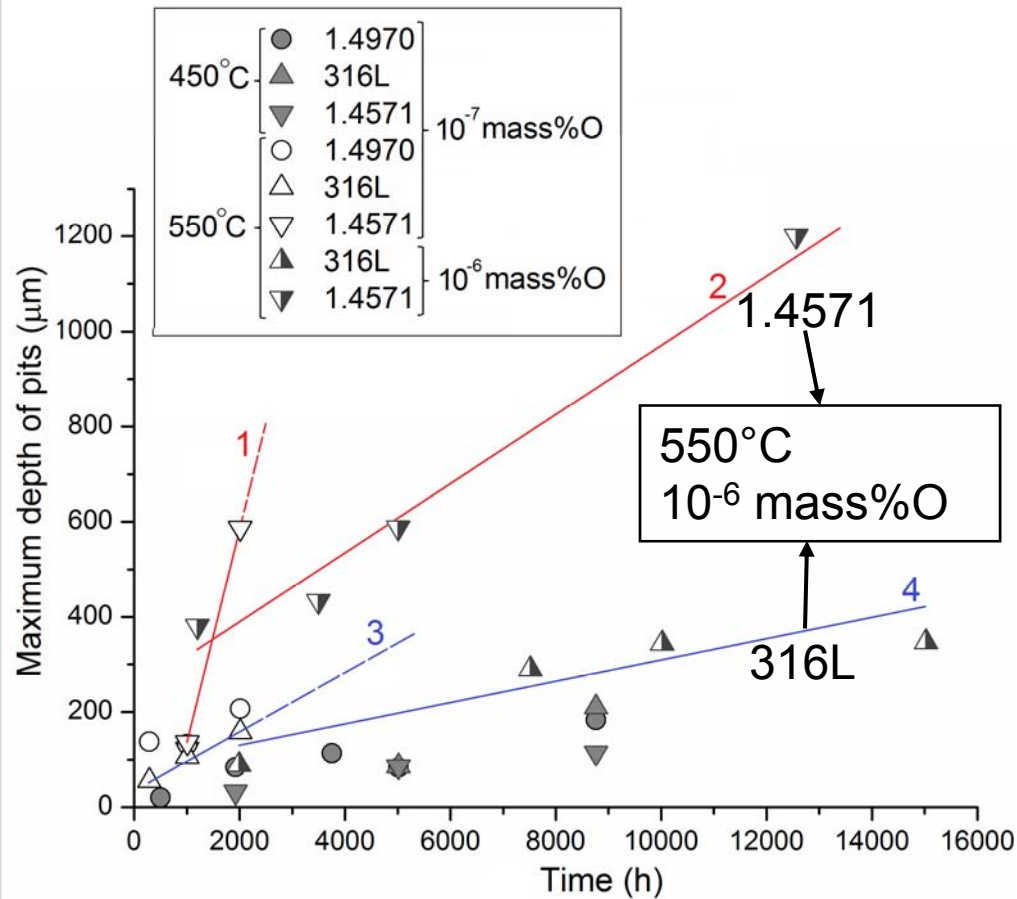
Surface appearance (%)	550°C				450°C						
	288h	715h	1007h	2011h	500h	1007h	1925h	2015h	3749h	5015h	8766h
1.4970											
Layer-type (L)	6	43	62	75	42	*	33	*	52	23	92
Pit-type (P)	5	-	35	16	9		46		44	11	8
(L + P)**	11	43	97	91	51		79		96	34	100
1.4571											
Layer-type (L)	4	46	68	42		*	17	*	100	4	98
Pit-type (P)	-	-	7	13			1		0	3	2
(L + P)**	4	46	75	55			18		100	7	100
316L											
Layer-type (L)	4	58	88	82				*	100	8	92
Pit-type (P)	4	-	8	9		*		*	0	7	8
(L + P)**	8	58	96	91					100	15	100

* - smooth surface covered by thin (~ 0.5 μm) protective Cr-based oxide film

** - L + P = selective leaching attack

☐ The percentage of surface affected by selective leaching attack increases with time

Comparison of results at 10^{-7} and 10^{-6} mass% O



Maximum depth of pit-type corrosion attack on austenitic steels tested in flowing LBE (~ 2 m/s) depending on temperature and oxygen concentration in the melt.

□ 10^{-6} mass% O – preferential oxidation (spinel);

□ 10^{-7} mass% O – preferential selective leaching;

□ At constant $C_{O[LBE]} \sim 10^{-7}$ mass% O, the depth of pits increases with temperature increasing from 450°C (solid symbols) to 550°C (open symbols);

□ At constant $T = 550^\circ\text{C}$, the maximum depth of pits increases when concentration of oxygen in the melt decreases from 10^{-6} to 10^{-7} mass% O;

□ Under the other similar conditions of test (550°C, $\sim 10^{-7}$ mass% O), the finer grains of steel the deeper corrosion attack: one can compare curves 1 in Fig. (fine grained 1.4571) and 3 (coarse-grained 316L) and curves 2 (1.4571) and 4 (316L) fitted for 550°C and concentrations of oxygen 10^{-7} and 10^{-6} mass% O, respectively.

Conclusions



- ❑ Austenitic steels (1.4970, 316L and 1.4571) showed complex corrosion behavior in flowing (2 m/s) LBE with 10^{-7} mass % O at 450 and 550°C. Interaction was accompanied by formation of a thin ($\leq 0.5 \mu\text{m}$) Cr-based oxide film characterizing the incubation period followed by the selective leaching of Ni and Cr from the sub-oxide layers resulting in development of general layer-type and local pit-type attack.
- ❑ **Cr-based oxide film, formed *in-situ* on the surface of austenitic steels, is not a sufficient protective barrier with respect to the selective leaching under the given conditions of test !!!**
- ❑ In the LBE with 10^{-7} mass%O the selective leaching is a main corrosion mechanism of austenitic steels causing substantial corrosion loss, while in LBE with 10^{-6} mass%O the oxidation prevails. The local deep corrosion attack due to selective leaching seems to be a critical factor affecting corrosion resistance of austenitic steels in oxygen-controlled LBE while oxidation is only postpones the unavoidable start of selective leaching.
- ❑ The residual surface pattern and stresses resulting from the mechanical preparation of samples (turning) in combination with local flow conditions facilitates the local breakdown of the oxide film. As the local corrosion attack initiated, the bulk structure of steel became dominant for its further development. In this case, substantial number of preferential diffusion paths, such as deformation twins (1.4970) and fine-grained structure (1.4571) characterized by high grain boundary density, both favor the selective leaching attack.

Acknowledgements



The construction and operation of the CORRIDA loop was financially supported by the Nuclear Safety Programme of KIT.

The presented work is part of the MATTER project that has received funding by the 7th Framework Program of the EU (Grant Agreement No. 269706).